MODELLING PARTICULATE FLOW DURING IMPREGNATION OF DUAL-SCALE FABRICS

V. Frishfelds and T.S. Lundström*
Division of Fluid Mechanics, Luleå University of Technology, SE-97187 Luleå, Sweden
*Corresponding author(staffan.lundstrom@ltu.se)

Keywords: *Manufacturing, particles, impregnation, dual-scale fabrics, modelling*

Summary

Filtration of particles during impregnation of dual-scale fabrics is studied numerically for a number of configurations with a previously derived model. The initial position and size of the particles are varied. The main result is that structural composites can be tailor-made as to additional properties by such an approach.

1 Introduction

Fabrics used in modern composite materials have often dual-scale porosity, < 10 μm inside the fibre bundles and > 100 μm between the bundles. The detailed geometry of such fabrics is, for instance, of importance for applications when the resin is doped with particles to create multifunctional composites, [1-3]. The added particles can, for example, enhance the fire resistance, toughen the material, introduce electrical conductivity and shielding properties to the material [4-7]. In order to achieve satisfactory properties of these functional materials, it is vital to have a known spatial distribution of the functionality throughout the material and it is of great interest to develop methods to control the distribution of particles during manufacturing. With a controlled particle distribution the functionality sought for can be optimized without sacrificing other properties. The model here described can be used to increase the understanding of particulate flow during manufacturing of structural composites as shown in [8]. We will here continue to demonstrate the capability of the model by studying the filtration of particles at fully saturated conditions for different size and position distributions of the particles.

2 Theory

The theory for the flow field is based on [9] and will shortly be repeated while the background to the motion of the particles was outlined in [10].

2.1 Flow field

Flow perpendicular to two-dimensional systems of fibres clustered in bundles is considered. Since the fibres themselves are impermeable to the fluid flow, the stream function at the surface of each fibre is constant according to $\psi = \psi_i$, where $i = 1\ldots n$ is the index of the fibres. The difference in stream function between any two fibres is determined by the flow rate in the gap between the two fibres in question. To derive the distribution of flow, the system is divided into n parts with a modified version of Voronoi diagram so that each part contains one fibre, see [8-10]. The fibres are assumed to be stationary and non-slip boundary conditions are applied. At the crossing between the centre to centre lines of fibres i and j with the Voronoi lines the value of the stream function and the vorticity $\boldsymbol{\omega} = \nabla \times (\nabla \times \boldsymbol{\psi})$ are denoted ψ_{ij0} and ω_{ij0}, respectively, see Fig. 1. Using this definition the quadratic average of vorticity in an area S_{ij} at fibre i adjacent to fibre j may be written as:

$$\left\langle \omega_{ij} \right\rangle = C_{ij} \frac{\psi_{ij0} - \psi_i}{d_{ij0}^2} \qquad (1)$$

where A_{ij} originate from the average vorticity in a small area S_{ij}; d_{ij0} is the distance between fibre i and the Voronoi line that separates fibres i and j; ~ denotes the case of equal sized fibres i and j. The total dissipation rate of energy approaches a minimum, [11], so the following sum over the total area should be minimised:

$$\Phi[\psi] = \tfrac{1}{2}\mu \int \omega^2 dS\,, \qquad (2)$$

where μ is the viscosity of the percolating fluid. The total sum is minimized with respect to all discrete

values of the stream function and the vorticity. The total force on each fibre is derived from the vorticity near the fibres and by accounting for the viscous and normal forces according to:

$$\mathbf{f}_i = \mu r_i \sum_j \boldsymbol{\tau}_{ij} B_{ij} \frac{\psi_{ij0} - \psi_{ij}}{d_{ij0}^2} \Delta\varphi_{ij} \,, \tag{3}$$

where B_{ij}:

$$B_{ij} = \frac{d_{ij0}^2}{\psi_{ij0} - \psi_{ij}} \left(\left\langle \omega_{ij}^{arc} \right\rangle - r_i \left\langle \left(\frac{\partial \omega}{\partial n} \right)_{ij}^{arc} \right\rangle \right) \tag{4}$$

is a dimensionless variable characterising the ratio between the average vorticity along the arc at the border of the fibres and difference of the stream function at the positions indicated, see Fig. 1. The sum of all drag forces equals the driving pressure difference if wall effects are neglected. Hence, the permeability **K** follows from Darcy law

$$\langle \mathbf{v} \rangle = \mathbf{K} \sum_i \mathbf{f}_i \Big/ \left[\mu \sum_{ij} S_{ij} \right] \tag{5}$$

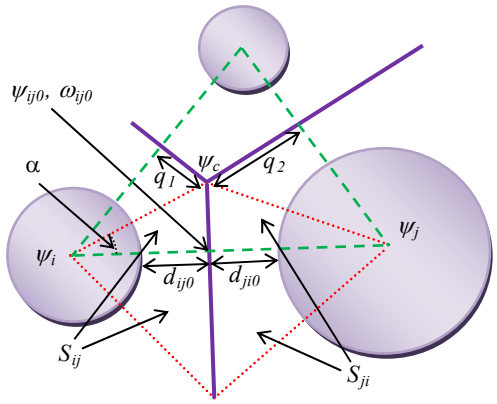

Fig. 1 –Modified Voronoi diagrams (solid), Delaunay triangles (dashed), and small triangles (dotted) between three fibres.

The dimensionless variables *A*, *B* in Eqn. 2-5 are obtained from simulations with Computational Fluid Dynamics (CFD). The simulations are carried out with boundary conditions representing a well structured repeatable material with varying geometry as described in [4].

2.2 Motion of particles

Following [8] the fibres are modelled to be stiff and stationary. The particles, in their turn, move with the fluid and redistribute with the flow field according to a quasi-stationary approach. It implies that the fluid flow and the corresponding Stokes drag force is calculated assuming that the particles at that moment are stationary implying that inertial effects are negligible but that the may have a major influence on the flow field. In next step the particles take new positions depending on the Stokesian drag force on the individual particles. The total force results from drag and friction according to:

$$\mathbf{f}_i^{fr} = k \frac{r_i^2}{\bar{r}_i^2} \mathbf{v}_i \,, \tag{6}$$

where k is coefficient characterising viscous friction.Particles are not allowed to move into each or into fibres. This, however, creates a contact force to another particle or to a fibre. Using the Monte Carlo Metropolis algorithm for relaxation of stresses, this force relaxes to equilibrium. Friction between bodies (particle-particle, particle-fibre) is not included because the bodies are always assumed to be separated by a tiny layer of fluid

Notice that we model a fully two-dimensional case and there is very little flow between two closely packed particles or between particles being located close to fibres. This differs from a three dimensional set of spherical particles where the flow often can, more easily pass. A consequence is that the fluid flow is more dependent on the fibre distribution in a two-dimensional case. A previous study on two and three dimensional systems shows that the dimension

influences the actual permeability level of random systems as well as the controlled distribution of local permeabilities, [12]. The same study also revealed that main trends of three dimensional systems can be captured using a two dimensional approach. The additional dimension makes it easier for the fluid to move around the particles, possibly providing a smoother result.

3 Modelling

A geometry mimicking three fibre bundles is constructed by randomising positions of fibres within imaginary ellipses; see the larger circles in Fig. 2 which also define the computational cell. The bundles with an initial porosity of 40% are placed in a stationary liquid resin and assumed to be fully impregnated with this resin. Now some of the resin is doped with particles as exemplfied with the smaller circles in Fig. 2, and the resin is subjected to a pressure gradient driving it from the top of the Figure to its bottom. Periodic boundary conditions are set on the top and bottom and on the side walls. Hence particles that leave the bottom boundary enter the top and particles leaving any of the side walls enter through the other. Three spatial distributions of particles are considered, i) At the inlet (and outlet) of the computational cell, ii) within the fibre bundles and a iii) a combination of i) and ii) as is the case in Fig. 2. In addition two sets of particle distributions are studied. For each set the size of the particles is randomised within certain limits to account for the variability of particle diameter. In the larger particle set the largest particle size is approximately half the average spacing between fibres in the bundles while in the smaller particle distribution the largest particle size is approximately a quarter of the average spacing between fibres.

4 Results and Discussion

Let us focus on the smaller particle distribution and start to discuss the result for the case when we initially have particles at the inlet and outlet of the cell and within the bundles, Fig 2. As the pressure gradient is applied most of the flow goes around the bundles implying that the stream function is almost constant for each bundle, see Fig. 2 where the colour of the particles and fibres denote the value of the stream functions for the current configuration. As the flow continues it can be observed that the particles outside bundles are not allowed to go inside the bundles, since the before-hand distributed intra-bundle particles reduce the permeability for flow through the bundle, see Fig 3. That is true both when particles are trapped in the channels formed between the bundles as is the case in the middle and right-hand side channels in Fig. 3 and when the are flowing with the resin as is the case for the left-hand side channel in Fig 3. As the particles are trapped in these channels the flow is nearly completely stopped and the distribution of stream function changes radically as shown by the colours in Fig. 3. However, some intra-bundle particles initially located near the boundary of the bundles can leave the bundle.

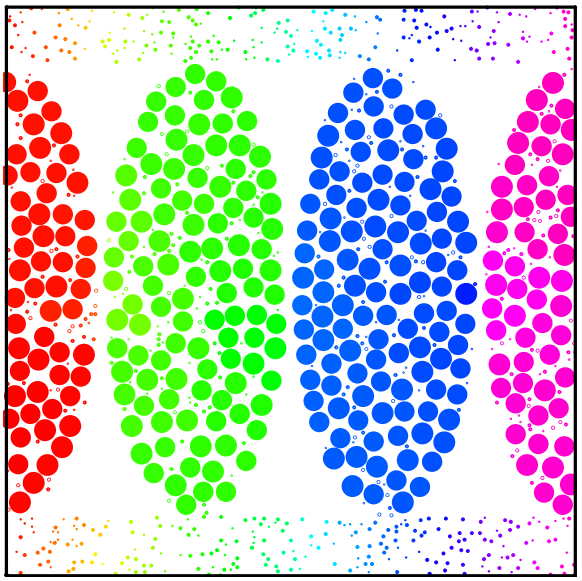

Fig.2. Initial configuration of fibre bundles and particles in a row (large circles). The flow is from the top of the figure to the bottom. Hollow small circles: particles initially inside the bundles; filled small circles – particles initially outside bundles. The colours indicate stream function.

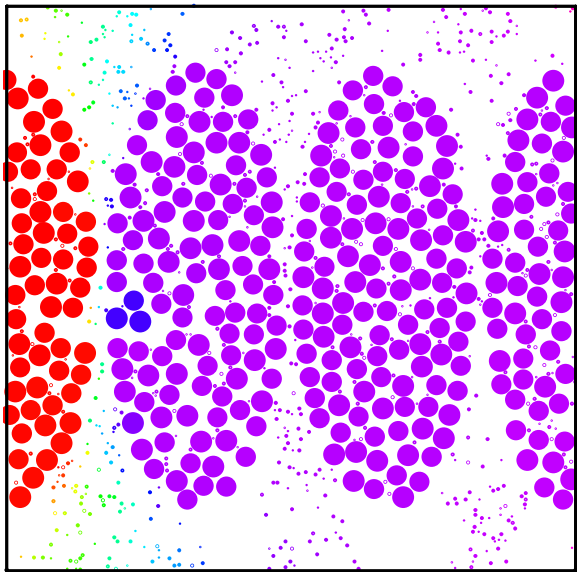

Fig. 3. A case when particles initially are placed both inside and outside bundles after a certain period of time as compared to Fig. 2.

The scenario is totally different for the case when there are initially no intra bundle particles. Then a large number particles move from the interbundle channels into the bundles especially at the top of bundles and at places where bundles touch each other. This type of motion becomes particularly apparent when the interbundle channels are blocked, see Fig 4 and the interbundle channels to the left and right. However, also some particles move from the middle channels where there is no blockage. The relatively extensive flow through the bundles is also mirrored by the wide distribution of stream function within the bundles. When the ratio between the particle diameter and the fibre diameter is decreased there is also a pronounced accumulation of particles at the top of the bundles, see Fig. 5. Then almost all tiny gaps at entrances of the bundles are sealed with the small particles. As a result the permeability of the system essentially reduces, see Fig. 6. Interestingly, a similar kind of sealing occurs when small base particles moves into larger filter particles [10]. The result is also in agreement with experimental observations in [3].

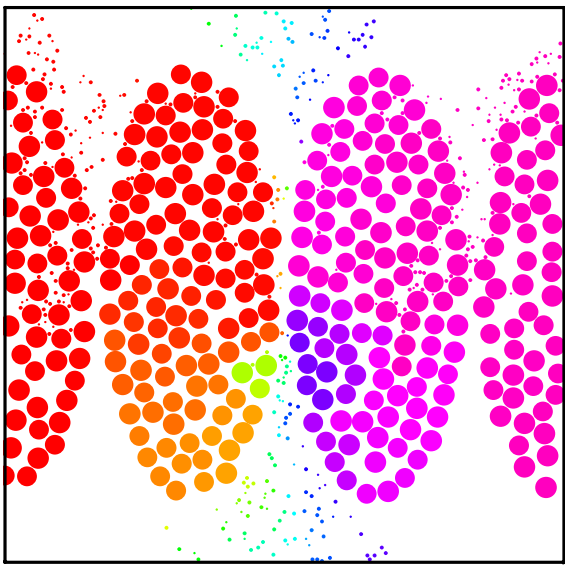

Fig. 4. A case when there initially are no particles within the fibre bundles.

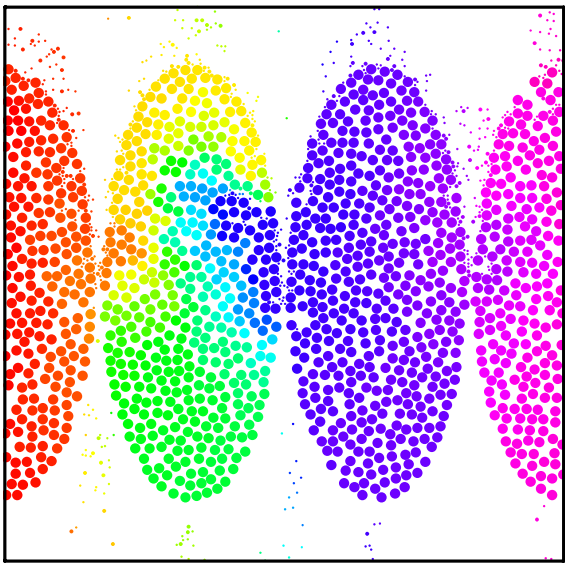

Fig. 5. A set-up as in Fig. 4 but with when the ratio between the particle diameter and the fibre diameter is decreased.

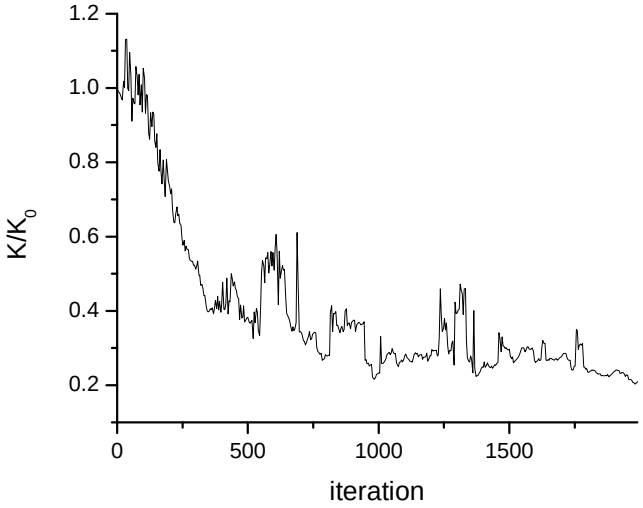

Fig. 6. Permeability for the set-up in Fig. 5.

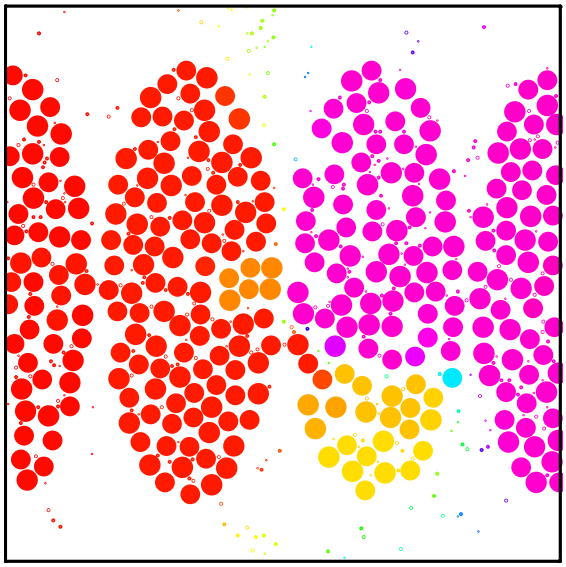

Fig. 7. A case when initially only particles inside bundles are present.

Yet another scenario is realised for the case where the particles were only located within the fibres bundles at the start of the flow. Particles close to the boundary of the bundles becomes free, while the others just move a bit to another place inside the bundle where they gets trapped, see Fig. 7. The overall motion of the intrabundle particles increases as the intrabundle channels are blocked which is the case in Fig. 7 for all channels. Due to this major streamlines goes through the bundles. Also for the case when the ratio between the particle diameter and the fibre diameter is decreased some of the intrabundle particles leave the bundles, see Fig. 8.

As shown we face very different scenarios dependent on where we initially place the particles which indicate that structural composites can be designed in detailed also on the micron and submicron level.

If the channels between the bundles are wider, then intense flow goes around all the bundles, see Fig. 9. As a result the intrabundle particles leave the bundles all around every bundle not just bundles with higher difference between the stream function values. It suggests that flow through the bundles is less important in both cases Fig. 8 and Fig. 9 and only intrabundle particles subjected to strong interbundle flow are liberated. Weak intrabundle flow occurs because the intrabundle particles essentially block the flow inside the bundle. This could change considering smaller particles in bundle with higher porosity, when the weak intrabundle flow could still free the particles after infinitesimally long time. Interestingly, that for wider channels as in Fig. 9 the permeability increases with time which is opposite to the results in the set-ups in Fig. 5-6. The reason to the increase is that the intrabundle particles near the channel move out of the bundles and the pressure gradient through this bottleneck of the flow is reduced at the same flow rate.

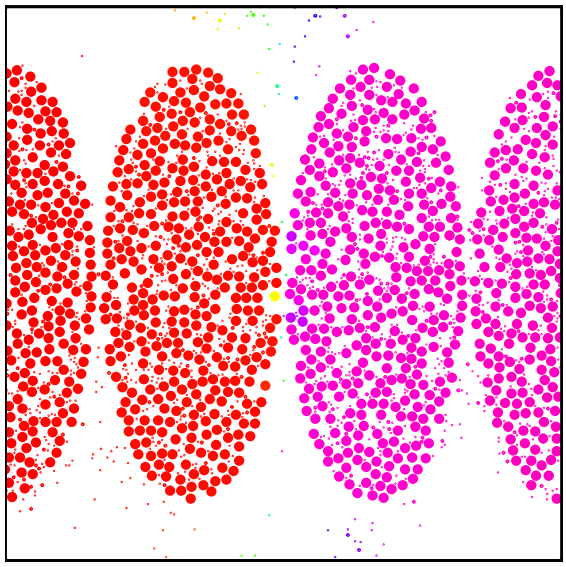

Fig. 8. The same set-up as in Fig. 7 when the ratio between the particle diameter and the fibre diameter is decreased.

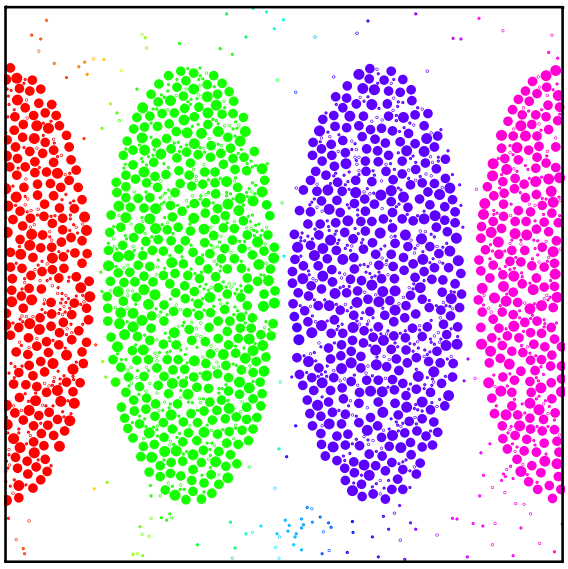

Fig. 9. The same set-up as in Fig. 8 when the gap between bundles is increased.

5 Conclusions

We have demonstrated the capability of a previous derived model and shown how structural composites can be tailor-made by altering initial position and size of particles added to the resin. In particular doping the fibre bundles with particles will result in that particles in the resin mainly move around the bundles. This effect may also be obtained by matching the size of the inter bundle particle diameter to the diameter of the fibres.

6 References

[1] Chohra, M., Advani, S.G., Gokce, A., Yarlagadda, S., "Modeling of filtration through multiple layers of dual scale fibrous porous media" , Pol. Comp. 27 (5), pp. 570-581 (2006)

[2] Fernberg SP, Lundström, T.S., Sandlund EJ, "Mechanisms controlling particle distribution in infusion molded composites". J. Reinf. Plas. Comp. 25:59-70 (2006)

[3] Nordlund, M. Fernberg, S.P. and Lundström, T.S., "Particle Deposition Mechanisms during Processing of Advanced Composite Materials", Composites: Part A, 38 (10), 2182-2193 (2007)

[4] Katerelos, D.T.G., Joffe, R., Labou, D., Wallstrom, L, "Alteration of the mechanical behaviour of polypropylene owing to successive introduction of multiwall carbon nanotubes and stretching", Mechanics of Composite Materials 45 (4), pp. 423-434 (2009)

[5] Mouritz, A.P., Feih, S., Kandare, E., Mathys, Z., Gibson, A.G., Des Jardin, P.E., Case, S.W., Lattimer, B.Y., "Review of fire structural modelling of polymer composites, "Composites Part A: Applied Science and Manufacturing", 40 (12), pp. 1800-1814 (2009)

[6] Lee, S., Jeon, Y.-P., "Effects of mixing on electrical properties of carbon nanofibre and polymer composites" Journal of Applied Polymer Science 113 (5), pp. 2980-2987 (2009)

[7] Sadeghian, R., Gangireddy, S., Minaie, B., Hsiao, K.-T., "Manufacturing carbon nanofibres toughened polyester/glass fibre composites using vacuum assisted resin transfer molding for enhancing the mode-I delamination resistance ", Composites Part A: Applied Science and Manufacturing 37 (10), pp. 1787-1795 (2006)

[8] Frishfelds, V., Lundström, T.S., "Modelling of Particle Deposition during Impregnation of Dual-Scale Fabrics" Plastics, Rubber and Composites: Macromolecular Engineering, 40 (2), 65-69 (2011)

[9] Hellström, J.G.I., Frishfelds, V., Lundström, T.S., "Mechanisms of flow-induced deformation of porous media" J. of Fluid Mech. 664, 220-237 (2010)

[10] Frishfelds, V., Hellström, J.G.I., Lundström, T.S., Mattsson, H., "Fluid flow induced internal erosion of porous media; Modelling of the No erosion filter test experiment" Transport in Porous Media Accepted (2011)

[11] L. Berlyand and A. Panchenko, "Strong and weak blow-up of the viscous dissipation rates for concentrated suspensions", Journal of Fluid Mechanics, Vol. 578, pp: 1-34 (2007)

[12] Lundström T.S., Frishfelds, V., Jakovics, A., "A statistical approach to permeability of clustered fibre reinforcements" Journal of composite materials, 38 (13), 1137-1149 (2004)